IUST
Iran University of Science and Technology

Iranian Journal of Electrical and Electronic Engineering

Journal Homepage: ijeee.iust.ac.ir

Research Paper

A Novel Protection Method for UPFC Compensated Transmission Line Based on Cooperative Game Theory

M. Khalili*, F. Namdari*(C.A.), and E. Rokrok*

Abstract: This paper presents a new single-end scheme to locate and protect faults on the compensated transmission line using the Unified Power Flow Controller (UPFC). The UPFC controllers have remarkable effects on the transient and steady-state components of the voltage and current signals. First of all, this study evaluates the impact of UPFC on Traveling Waves (TW) that pass through the UPFC location. Following that, the effects of UPFC's harmonic on conventional protections will be investigated using the TW theory. A single-end method will be presented in the next stage to protect and locate the faults on the compensated transmission lines with UPFC. Moreover, an extraction technique (i.e., Discrete Wavelet Transform [DWT]) is used to process the current and voltage signals. As a branch of mathematics, cooperative game is employed in this study to represent the strategic interaction of different players in a context by predefined rules and outcomes. Additionally, this study made use of this theory to distinguish the extracted TWs from each other. The proposed method is assessed considering different fault situations with great variations in operating conditions accompanied by a UPFC placed at the midpoint of the line.

Keywords: Cooperative Game, Protection, Transmission Line, Traveling Wave, UPFC.

1 Introduction

TRANSMISSION lines (TL) have been recently designed for extensive power transfer capability. The FACTS Device can be regarded as a flexible approach to provide an exclusive combination of rapid compensation by series and shunt devices. The UPFC introduces a new area for the system parameter control (bus voltage, as well as active and reactive power). The utilization of this device increases the system stability, improves transferring capability of the power, and other problems occurring during power system protection [1]. However, the UPFC in the fault loop has significant effects on the steady-state and transient components of current and voltage signals [2]. The UPFC implementation in TLs proposes new novel issues concerning the power system protection. In particular, the evaluation of the rapid changes in power angle, load current, TL impedance, and transient should be included in TL protection with respect to the fault occurrence and the control system performance. Additionally, since UPFC controllers have a very fast response time, it might overlap with the protective device time operation. The UPFC derives maximum advantage when sited at the mid-point of the TL [3]. The findings obtained by [4] and [5] revealed the negative effects of the midpoint series and shunt-FACTS devices on the distance relay performance.

The TWs that are generated as a result of fault occurrence in a TL, travels to both sides of the power line. These TWs provide information about the location, direction, and type of the fault which have been utilized to introduce protection schemes with a high speed [6]. Moreover, TW-based protection schemes have much less operation time, compared to conventional ones. The researchers have been interested in evaluating the TW-based protection. As a result of advances in technology and increasing progression in signal processing, there have been significant improvements in the applicability and reliability of TW-based protection methods; however, it should be noted that these schemes require

Iranian Journal of Electrical and Electronic Engineering, 2022.
Paper first received 05 January 2021, revised 20 March 2021, and accepted 07 April 2021.
* The authors are with the Department of Electrical Engineering, Engineering Faculty, Lorestan University, Khoramabad, Iran.
E-mails: khalili.mehrdad90@gmail.com, namdari.f@lu.ac.ir, and rokrok.e@lu.ac.ir.
Corresponding Author: F. Namdari.
https://doi.org/10.22068/IJEEE.18.1.2082

high-frequency bandwidth equipment [7].

Different schemes are introduced to detect and classify the faults in the UPFC compensated TLs employing TW. In this regard, [8] employed wavelet combined entropy in an efficient time-frequency analysis for fault classification and section identification in UPFC compensated TL by current signals and post-fault voltage. Furthermore, [9] detected and classified faults in a double-end UPFC compensated TL using a fuzzy logic approach and combined wavelet. Nevertheless, global positioning system (GPS) time-stamped synchronized current signals are required in this method at both ends of the TL to fulfill the fault detection and classification tasks. In the same line, wavelet singular entropy (WSE) was used by [10] to propose the fault detection and classification method for UPFC compensated TL. In this method, the summation of the 4th level detail coefficients and the WSE of three-phase currents are used to detect and classify the faults, respectively.

It is of utmost importance to investigate the effect of UPFC on TW-based protection. Since there is a dearth of studies on the effect of FACTS devices, the purpose of this paper is to investigate the impact of UPFC on these protection methods. Moreover, it attempts to provide solutions in case of any problems.

Using the TW theory, the present study aims to evaluate the effect of UPFC on a conventional protection scheme. For this purpose, the first section of this paper is allocated to the investigation of UPFC effect on TWs passing through a connection point of UPFC. The second part of this study evaluates the effects of generated transients during faults resulted from UPFC's harmonic. The obtained results demonstrated the probability that TW is being reflected from the UPFC location. Furthermore, the other transients developed by UPFC's harmonic during fault occurrence resulted in the generation of TWs. The amplitude of the first TW reflected from the fault point is similar to that of these TWs. The single-ended protection schemes identify the reflected TW from the fault point relying on the threshold based on the TW. The poor performance of the single-end protection schemes is notably due to the disturbance from the UPFC. Therefore, this paper aims to propose a single-end protection method based on TWs using cooperative game. Furthermore, the present study utilized this theory owing to an access to select the low threshold in identifying the reflected TWs. It should be noted that this theory can distinguish the identified TWs. The obtained results confirmed that the algorithm was not affected by various fault inception angles, different locations, and types of faults.

2 Basic Concept

2.1 UPFC Model and Modes of Operation

As a combined series-shunt FACTS device (STATCOM AND SSSC), the UPFC includes two back-to-back converters that are connected through a common DC link as illustrated in Fig. 1. At the sending side, the first VSC is connected in a shunt, and the second VSC is connected in series with the TL. The shunt and series coupling transformers (T_{se} and T_{sh}) are used to connect these converters to the TL. Moreover, the voltage magnitude of the bus (j_1) and power flow via TL (j_1, j_2) can be controlled using the UPFC. The equivalent circuit of UPFC is usually shown as shunt and series voltage source (Fig. 1) [11].

3 Impact of UPFC on the Protection Based on TW Theory

3.1 Protection Based on TW

The TWs are propagated to the ends of the TL by the electrical disturbances. In each disturbance, these TWs are generated and contain high-frequency signals, which propagate from the disturbance point towards the TL. At a discontinuity point, part of the TW is reflected, and the rest is transmitted owing to various impedances present at the junction [12]. Assume a fault in the TL occurring in front of the UPFC. Fig. 2(a) displays the pre-fault conditions on the TL, in which e_f signifies the pre-fault voltage. Superimposition on the pre-fault network voltages and currents produced by a fault can be employed to simulate the fault occurrence. This incorporates a single source of magnitude $-e_f$ at the fault

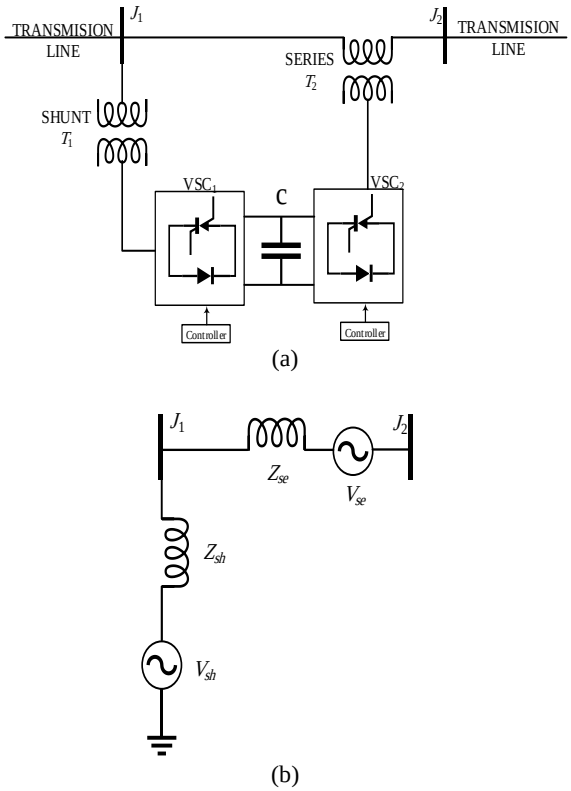

Fig. 1 a) UPFC compensated transmission system and b) Equivalent circuit of UPFC [11].

location. The network voltage can be divided into a sinusoidal voltage with a constant frequency and two TWs with respect to the fault occurrence conditions. These approximately rectangular parts contain a magnitude of $-e_f$ propagating away from the fault location.

These TWs which are reflected in any discontinuity involve the terminal that is connected to the UPFC. If the TWs conflict the discontinuity, part of the TW is reflected in the TL, and the rest continue their ways.

As can be observed in Fig. 3, a TW is generated in TL A and travels to UPFC. Following that, a part of the incident TW that reaches the J_1 breakpoint is reflected, and the other fraction is transmitted to the UPFC. Furthermore, as the transmitted TW reaches J_2, a part of the TW is expected to be reflected due to the changes in the impedance that are ahead of the TW. The rest will be transferred to TL B, and the V_4 is the first TW that is impressed on TL B. Furthermore, the reflected TW (i.e., V_3) reaches J_1 again, and part of it is reflected (V_5) and travels to the J_2 breakpoint. In the UPFC, this scenario occurs several times, and eventually, the losses attenuate the TWs reflected in the UPFC. It is worth mentioning that instant occurrences of the refraction and reflection scenarios can be observed in UPFC. Moreover, no time interval can be considered for the reflected and transmitted TWs.

The UPFC equivalent circuit is usually demonstrated as shunt and series voltage sources (Fig. 1(b)). In this figure, Z_{se} indicates the series impedances and Z_{sh} presents the shunt coupling transformers [11].

In the following, the refraction and reflection coefficients are presented assuming the compensation of the TL by UPFC. Where, V', I' signifies the incident TW, and V, I presents the transmitted TW. Moreover, V'', I'' is the reflected TW, and ρ denotes the reflection or refraction coefficient.

Following that, the discontinuity point (UPFC) incorporates a series and shunt inductor with L_{se} *and* L_{sh} capacity, respectively.

Using Laplace transform, a transmitted and reflected TW yields:

$$V' = \frac{1}{s} \tag{1}$$

$$v_4(s) = \frac{4}{s\left(\frac{1}{L_{se}.s} + \frac{1}{L_{sh}.s} + \frac{1}{z}\right)\left(L_{se}.s + z\right)} \tag{2}$$

$$v_6(s) = \frac{4\left(\frac{1}{L_{se}.s} - \frac{1}{L_{sh}.s} - \frac{1}{z}\right)\left(-L_{se}.s + z\right)}{s\left(\frac{1}{L_{se}.s} + \frac{1}{L_{sh}.s} + \frac{1}{z}\right)^2\left(L_{se}.s + z\right)^2} \tag{3}$$

The inverse Laplace transform for the impressed voltage on TL B yields (4) as follows:

$$v_4(t) = 4\left(\frac{e^{-\frac{tz}{L_{se}}}L_{sh}}{L_{se}} - \frac{e^{-\frac{t\left(L_{se}.z + L_{sh}.z\right)}{L_{se}Lsh}}L_{sh}}{L_{se}}\right) \tag{4}$$

$$\begin{aligned} v_6(t) = 4\Bigg(&\frac{e^{-\frac{tz}{L_{sh}}}\left(L_{se}{}^2L_{sh} - 8L_{sh}{}^3\right)}{L_{se}{}^3} \\ &+ \frac{e^{-\frac{t\left(L_{se}.z + L_{sh}z\right)}{L_{se}.L_{sh}}}\left(-L_{se}{}^2L_{sh}{}^2 + 8L_{sh}{}^4\right)}{L_{se}{}^3L_{sh}} \\ &- \frac{2e^{-\frac{tz}{L_{se}}}t\left(L_{se}.L_{sh}z - 2L_{sh}{}^2z\right)}{L_{se}{}^3} \\ &+ \frac{2e^{t\left(-\frac{z}{L_{se}}-\frac{z}{L_{sh}}\right)}t\left(L_{se}L_{sh}{}^3z + 2L_{sh}{}^4z\right)}{L_{se}{}^3L_{sh}{}^2}\Bigg) \end{aligned} \tag{5}$$

Considering no significant time interval between TWs V_4 and V_6, these two TWs can be added together that leads the TW to pass through the UPFC.

$$v_{transmitted\ wave}(t) = \frac{8e^{-\frac{(L_{se}+L_{sh})tz}{L_{se}.L_{sh}}}}{L_{se}{}^3}L_{sh}\left[\left(-1+e^{\frac{tz}{L_{sh}}}\right)L_{se}{}^2 - \left(-1+e^{\frac{tz}{L_{sh}}}\right)L_{se}tz + 2L_{sh}\left(-2\left(-1+e^{\frac{tz}{L_{sh}}}\right)L_{sh} + \left(1+e^{\frac{tz}{L_{sh}}}\right)tz\right)\right] \tag{6}$$

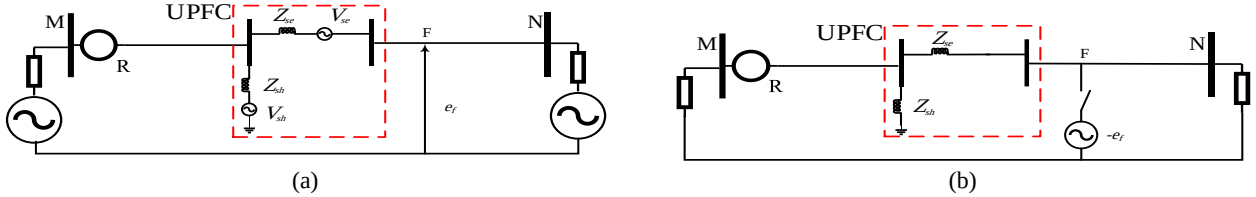

(a) (b)

Fig. 2 A single-phase schematic compensated TL. TW propagation is initiated by a fault; a) Initial conditions and b) Fault representation.

$$\rho_{refraction}(s)=\frac{8L_{se}.L_{sh}sz\left(L_{sh}z^{2}+L_{se}^{2}s\left(L_{sh}.s+z\right)\right)}{\left(L_{se}.s+z\right)^{2}\left(L_{sh}.z+L_{se}\left(L_{sh}.s+z\right)\right)^{2}} \quad (7)$$

The reflected TW is equal to (8) at point J_1.

$$v_{Reflected\ wave}(t)=e^{-\frac{(L_{se}+L_{sh})tz}{L_{se}.L_{sh}}}\frac{1}{L_{se}^{2}}\left(-e^{\frac{(L_{se}+L_{sh})tz}{L_{se}.L_{sh}}}L_{se}^{2}+8L_{sh}^{2}-2e^{\frac{tz}{L_{sh}}}\left(-L_{se}+2L_{sh}\right)\left(L+2L_{sh}-2tz\right)\right) \quad (8)$$

$$\rho_{reflection}(s)=\frac{1}{\left(L_{se}.s+z\right)^{2}\left(L_{sh}.z+L_{se}\left(L_{sh}.s+z\right)\right)}\times\left[L_{se}\left(3L_{sh}.s-z\right)z^{2}-L_{sh}.z^{3}+L_{se}^{3}s^{2}\left(L_{sh}.s+z\right)-L_{se}^{2}sz\left(3L_{sh}.s+4z\right)\right] \quad (9)$$

Fig. 4 displays the reflected and transmitted voltage TWs. At the initial moment, the reflected and transmitted TWs curves signify the refraction and reflection coefficients (0 and 1, respectively). Moreover, a small part of the TW that is transmitted to TL B can be indicated by the voltage curve transmitted in TL B. On the other hand, the reflected wave curve signifies that the TW which is reflected towards the source of the TW at final and initial moments is accompanied by –1 and 1 coefficients, respectively.

Fig. 5 displays that the refraction and reflection coefficients are in the frequency domain. Considering the high-frequency TWs, the refraction and reflection coefficients are close to 0 and 1 which are shown by the curves, respectively. Therefore, in the TL, high-frequency TWs may be attenuated or distorted.

Based on the findings obtained from the curves, a noticeable fraction of the high-frequency TW is reflected. At the UPFC location, reflections can challenge TW-based protection schemes. This leads to an inaccurate performance when the aim is to detect the first successive TW reflected from the fault point.

3.2 TWs and Harmonic

The UPFC contains two voltage source converters (VSCs) based on GTO that are connected through a DC capacitor link. A 6-pulse VSC is a basic voltage convertor model with a large number of harmonics; accordingly, its output voltage is not sinusoidal, and the generated output voltage involves the harmonics of $6n\pm1$ order (i.e., 5th, 7th, 11th, and 13th). The total harmonic distortion (THD) of the VSC output voltage is estimated around 30%, which does not meet the criteria of the IEEE 519 standard. The combined output voltage consists of the harmonics of $12n\pm1$ order (i.e., 11th, 13th, 23rd, and 25th) in the 12-pulse VSC. Furthermore, the generated output voltage involves the harmonics of the $48n\pm1$ order (i.e., 47th and 49th) with respect to the 48-pulse VSC. Accordingly, the THD is around 4% in the voltage, which satisfies the IEEE 519 standard [13, 14]. Table 1 summarizes the voltage THD of the voltage source converter.

The UPFC generates harmonic voltages during normal operation. Additionally, there are concerns that these signals may disrupt the structures of the TW that are utilized by relays during a fault. As a result, to reduce or

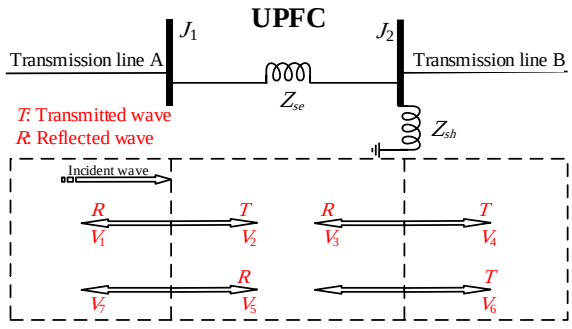

Fig. 3 Circuit diagram for a compensated TL with UPFC.

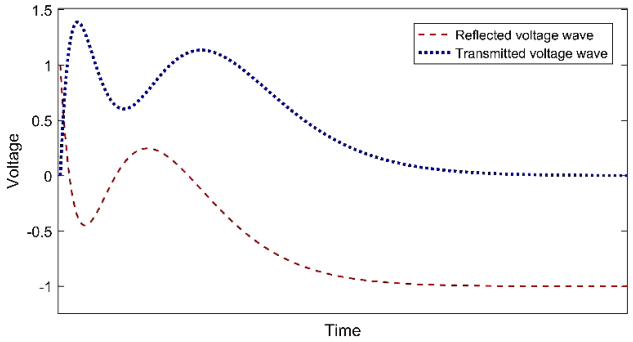

Fig. 4 Transmitted and reflected voltage TW across the UPFC.

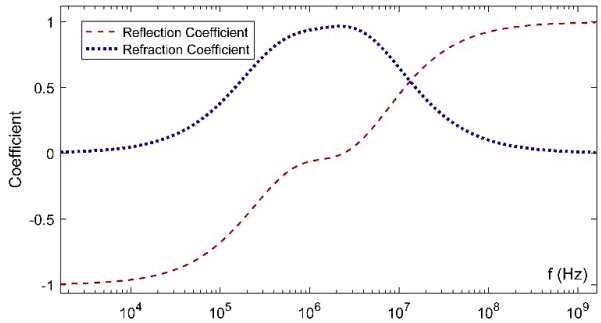

Fig. 5 Refraction and reflection coefficient.

Table 1 standard voltage THD of two-level VSC [14].

Pulse number of VSC	6	12	18	24	30	36	42	48	96
%THD	30.9	15.2	10.1	7.5	6.1	5.4	4.3	3.75	1.8

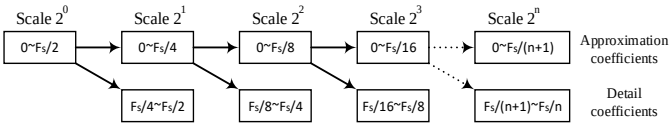

Fig. 6 Frequency band decomposition by DWT [15].

delete the distortion risk in the TW pattern, it is proposed to separate the low from high-frequency signals as a practical approach. In this technique, DWT and proper detail (cD_n) can be employed, and n is considered the level of decomposition [15]. This paper used the mother wavelet db4 [3].

In the DWT, each decomposition level is related to a wideband, which relies on the frequency of sampling in the time domain. Fig. 6. illustrates the wideband for the detail coefficients cD_n. Considering a 1 MHz sampling frequency, harmonic frequencies generated by the 48-pulse UPFC are close or inside the cD_5, cD_6, and cD_7 frequency bands. Therefore, $cD_{5\text{-}7}$ cannot be employed for TW protective relaying. Therefore, the bandwidth employed for relaying must be remarkably higher than the frequencies of the harmonics that are generated by the UPFC.

As shown in Fig. 7, a three-phase fault was applied at 250 km from the local end to show the practical effect of harmonic voltages generated by the UPFC. Moreover, Fig. 7 shows the detail coefficients of cD_{1A} and cD_{6A} obtained after applying the DWT (alpha mode of measured current).

Considering Fig. 7, the calculated TWs can be discriminated using cD_{1A}. On the other hand, after the fault event, the calculated TWs using cD_{6A} are disrupted significantly (Fig. 7). This distortion is caused by the frequencies of the harmonic voltage that are produced by the UPFC inside the cD_{6A} bandwidth (Fig. 6), thereby resulting in a significant interaction. The utilization of cD_{1A} instead of cD_{6A} in this particular case can lead to the better detection and discrimination of the high-frequency TWs resulting from a fault event.

4 The Proposed Protection Scheme Based on TW Theory

Fig. 8 illustrates the flowchart of the proposed protection scheme using the TW theory. High-frequency digital relay measurement units are employed in this scheme to sample the current signals and voltage of all phases (n = 3). Furthermore, after sampling, the coupling effect among the phases was minimized using a modal transform, and various techniques, such as mathematical morphology filter (MMF) [7], DWT [3], differentiator smoother filters [16], and Park's Transformation [17], utilized in this study can be employed to extract the TWs from the signal mode α. DWT [3] was used in this study to evaluate the proposed scheme efficiency. According to the findings in [3], the wavelet Daubechies 4 (db4) detected the fast transients accurately in the power system. Therefore, detail 1 and Daubechies 4 are used by the wavelet transform to process the signals.

References [18] and [19] have proposed an algorithm to protect the TLs compensated by SVC and TCSC in the middle of the TL. According to the analysis in this study, UPFC has different effects on the performance of protection systems based on TWs due to the switching frequency and the way it is connected to the network. The switching frequency of UPFC is much higher than that of the SVC and TCSC. Therefore, the harmonics produced by the UPFC during fault and normal conditions can have a detrimental effect on fault-induced TWs and incident TW detection. However, because of the low switching frequency in SVC and TCSC, the harmonic of this device had no negative effects on the TWs protection. Furthermore, the UPFC is placed in the circuit in the form of series; accordingly, the results of the outputs show that the reflection coefficient of the UPFC connection point is higher than that of the SVC and TCSC. The reason for this is the presence of the T_{se} series inductor, which shows a high impedance for high-frequency TWs so that it reflects the front-wave using factor of 1. The TCSC is also placed in the circuit in the form of series; however, its equivalent circuit consists of a capacitor and a parallel inductor resulting in a smaller reflection coefficient. The presence of high-frequency harmonics in UPFC-compensated TLs requires the proposed algorithms to use high sampling frequencies for protection based on

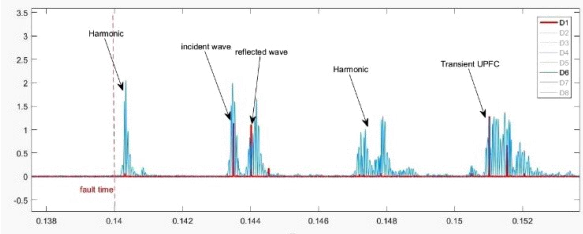

Fig. 7 Detail coefficient of cD_1 and cD_6 for a 3Ph fault (current).

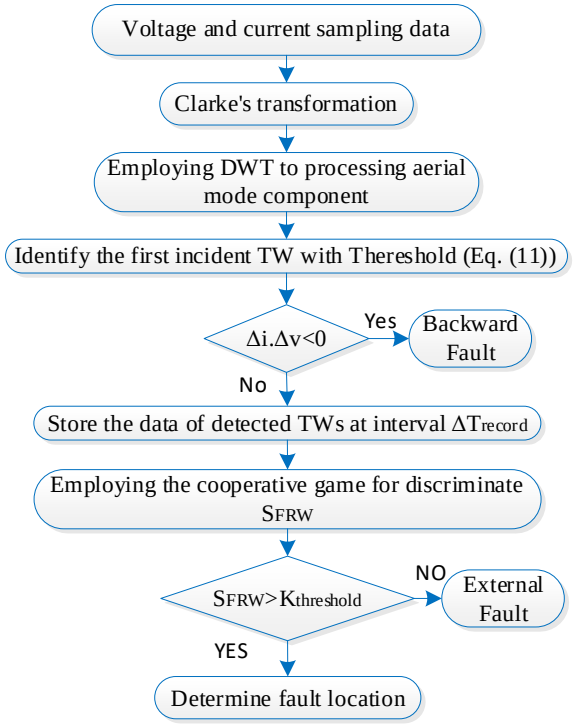

Fig. 8 Flowchart of the proposed protection scheme.

the TWs. Moreover, due to the high reflection coefficient of UPFC location, the proposed algorithms by [18] and [19] face challenges regarding the identification of the external fault and S_{FRW}, which shows no reliable performance. As a result, this paper utilized TW polarity to propose a single-end method to protect the UPFC-compensated TL.

The processed signals should be compared with the thresholds in order to identify the first incident TWs on TLs. Generally, the discarded TWs are the identified TWs that incorporate magnitudes smaller than the predefined threshold [16].

4.1 External Fault

Using $\Delta T_{reccord}$ intervals, all available TWs can be detected, thereby storing the data related to time, amplitude, and polarity. The reference time is the time of the first incident TW. According to the TW theory, the opposite polarity of the arriving voltage and current TWs is present when a forward fault occurs. However, regarding the backward fault, the arriving voltage and current TWs have the same polarity.

In the proposed method, the time required to store the TW data after the incident TW identification should be equal to $\Delta T_{reccord}$.

$$\Delta T_{record} = \frac{2L_{line} + 2L_{adjacent}}{v} \tag{10}$$

This study employs the identified current TWs polarity and amplitude S_{FRW} and incident TW in order to distinguish fault between internal and forward external fault. S_{FRW} corresponds to the first successful reflection of the incident TW from fault point.

When a fault occurs at the adjacent TL, the amplitude of the S_{FRW} is quite small since it gets attenuated at the busbar N twice. However, for a fault at the protected TL, S_{FRW} has considerable value. For the external and internal fault, this TW has small and large values, respectively.

On the other hand, this TW has opposite polarity as incident TW. Therefore, the polarity and amplitude of the S_{FRW} can discriminate the external fault.

The current (I) wave after traveling a distance x is equal to [20]:

$$I = I_0 e^{-\alpha x} \tag{11}$$

$$\alpha = -\frac{r + gZ_0^2}{2Z_0} \tag{12}$$

$$Z_0 = \sqrt{\frac{L}{C}} \tag{13}$$

where r, L, C, and g as the parameters per unit length of an TL and I_0 as the current wave at first of TL, and Z_0 is surge impedance of the TL. The S_{FRW} amplitude current wave will be equal to that in (14). In this paper, the $K_{threshold}$ coefficient is defined according to (15). In case the amplitude of S_{FRW} is greater than the $K_{threshold}$, the fault occurs in adjacent TL.

$$I_{S_{FRW}} = I_{incident} \, e^{-2V \cdot t_{FRW} \cdot \alpha} . K_{ref\_UPFC}^2 \tag{14}$$

$$K_{threshold} = K_{ref\_FP} \left| I_{incident} \, e^{-2.L.\alpha} . K_{ref\_UPFC}^2 \right| \tag{15}$$

where K_{ref_bus} is the reflection coefficient estimation of the busbar N. Moreover, K_{ref_UPSC} and K_{ref_FP} denote refraction coefficient of the connection point of UPFC and reflection coefficient of the fault point, respectively. In this paper, K_{ref_FP} is equal to 0.8 (high resistance fault).

4.2 Fault Location

Assume that UPFC compensates the TL M-N at the midpoint of the TL (Fig. 2). Following that, the directed relay R is placed at busbar M to protect the TL (M–N). At the relaying point, the current that flows from busbar M into busbar N results in a positive direction. Based on the TW theory the scenarios to protect the compensated TLs include the faults at the first and second half of a TL.

Let's assume a fault at the first half of the TL (Fig. 9(a)). After the identification of the first incident TW, a reflected TW in the voltage and current signals is received from the positive direction. The fault location can be calculated by identifying the e_{r1} and e_{r2} TWs. There are other TWs in addition to the TWs that are induced by faults and propagated along with the TL, which can disrupt the fault location and detection schemes. A fraction of the TW e_{f1} propagates to busbar N. Following that, it is reflected when it reaches the busbar J_1, and the rest continues along with the TL. According to Section 3. Refraction and reflection coefficients are calculated, and a part of the TW e_{f1} is

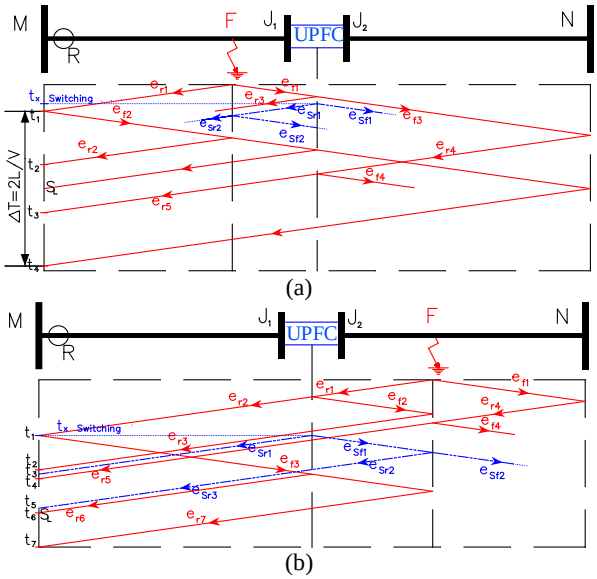

Fig. 9 Bewley lattice diagram; a) Fault before the UPFC location and b) Fault after UPFC location.

reflected to the fault point (e_{r3}). Since the reflection coefficient value of the fault point is higher than its refraction coefficient, a tiny part of this TW (e_{r3}) propagates towards the busbar *M*. On the other hand, the TL loss attenuates this negligible portion. Accordingly, in all modes of the UPFC, no TW resulted from a busbar (J_1) reflection reaches the busbar *M* with significant amplitude.

A similar Bewley lattice diagram of the TWs is illustrated in Fig. 9(b) with regard to the fault that occurs after the UPFC location. At the relay *R* location, other TWs can be observed along with the first incident and first reflected TWs (e_{r2}, e_{r7}) due to the fault. A part of the TW (e_{r1}) is reflected and travels to the fault point as TW e_{r1} passes through the UPFC. A great portion of the TW e_{f2} is again reflected and propagated to the busbar *M* due to the high reflection coefficient of the fault point. This is visible at the t_2 moment by the relay *R*. A TW can be observed at the t_4 moment as the fault occurs with resistance owing to the reflection of the TW e_{f1} at busbar *N*.

Another randomized TW that may be present is the GTO operation of the UPFC during a fault. Considering the condition that at the t_x moment, a transient wave is produced in the UPFC, the backward TW (e_{Sr1}) and the forward TW (e_{Sf1}) reflection from the fault point make the two TWs in t_3 and t_5 moments reach the relay location.

It is worth mentioning that the interval between t_3 and t_5 is twice the distance of the fault to the UPFC. A TW is observed at $t_6 = L/V$ for all the faults that occur in the second half of the TL. This is due to the reflection of the e_{f3} TW at the J_1 junction point.

The location of the fault can be obtained utilizing the equation below.

$$FL = \left(t_{FRW} - t_{First\ incident\ TW}\right) \times V \tag{16}$$

4.2.1 Discriminate the Identified TWs

Different numbers of TWs are detected in ΔT_{record} intervals by relay *R* that are consistent with the analysis in this section. To distinguish the identified TWs, the proposed single-end protection scheme used the Cooperative game. In this study, t_n and A_n signify the time and amplitude of n^{th} TW, respectively. d_{com} is compensation distance from the local end. Furthermore, EF_i represents the estimated fault location and *L* is the length of the TL. The FL indicates the fault distances from the *M* bus, and t_i^A denotes the approximation time of the first reflected TW from the fault point (S_{FRW}).

4.3 Cooperative Game

Game theory is a rational decision-making process among strategic participants. They follow the best payoffs for themselves and take into account the interaction of their profits among others and their abilities to collect data [21]. This mathematical tool has been used in power systems since it can solve decision-making problems involving multiple objectives and entities. Therefore, this paper aimed to employ the "Cooperative game" to discriminate between the identified TWs.

4.3.1 The Cooperative Game to Discriminate the TWs

Cooperative games allow the players to notice how the players can obtain a motif to make decisions independently. Players collaborate as any entity to enhance their payoff in a game. Each group of players is called a coalition (*C*), and the coalition of all players is regarded as a greater coalition. The cooperative game consists of a set of players $N = \{1, 2, \ldots, n\}$, a set of actions S_i ($i \in N$) (for each coalition), and preferences over the set of all actions of which she/he is a member (for each coalition) [22]. Assume $N = \{1, 2, \ldots, n\}$, then, the characteristic function of the cooperative game with *n* players is a real-valued function *v*, $v: 2^N \rightarrow \mathbb{R}$. This satisfy $v(\phi) = 0$. *V* and (*C*) refers to the largest payoff that players can obtain via cooperation. A coalition structure of the finite players *N* is a pair (N, $\mathcal{C}$), where $\mathcal{C} = \{C_1, C_2, \ldots, C_m\}$, $1 \le m \le n$, satisfying $\bigcup_{k=1}^{m} C_k = N$; $C_i \cap C_j = \emptyset$, $\forall i, j \in \{1, 2, \ldots, m\}$, $i \ne j$ and $\mathcal{C}$ is called a partition of *N*. A cooperative game with coalition structure is a triple (N, v, $\mathcal{C}$), whose payoff vector is a list of real number $x_i\ (i \in N), X\ (N, v, \mathcal{C}) = \{x_i \in \mathcal{R} \mid \sum_{j \in C} x_j = v\ (C),\ \forall C \in \mathcal{C}\}$, and it can be observed that $\mathcal{C}$ is individual and rational if only $x_i \ge v\ (i),\ \forall i \in N$ [23].

A) Game Player

The detected TWs in the time interval of ΔT_{record} are regarded as players in this game after detecting the first incident TW that is induced by the fault.

$$N = \{TW_1, TW_2, \ldots, TW_n\} \tag{17}$$

B) Set of Action

There are seven actions in this game (i.e., *A*, *B*, *C*, *D*, *E*, *F*, and *G*), and each player has a role the meanings of which are explained below.

$$S = \{A_j, B, C, D, E, F, G\} \tag{18}$$

where A_j, *B*, and *C* denote the reflected TWs from the UPFC location (busbar J_2), far-end (busbar *N*), and a fault point, respectively. Moreover, *D* is the second reflected TW from fault point (S_{SRW}), *E* signifies the reflection of the incident TW by both ends of the overhead TL (S_{2L}), *F* is the reflection of the incident TW between the local end and UPFC location (S_L), and *G* presents no action. Considering the conditions, each

player can only have a role in each game. In any game, only one player can select the *A*, *B*, and *C* roles. Furthermore, in each game, role *C* must be selected by one of the players.

Each player causes an outcome (u_i) regarding his role. To evaluate the consequences of the role each player has, the following relationships should be taken into account.

Role A_j demonstrates that the TW (player) is generated due to the reflection occurring between the fault point and the busbar J_2. Assume the role of A_j for the i^{th} TW, then, the time of the S_{FRW} equals 19), and the polarity of this TW is opposite to that of the incident TW polarity for the first reflection. The second reflection (A_2) has the same polarity as the incident TW.

$$t_i^A = \frac{\Delta T}{2} + \frac{2.d_{com}}{j.V} \tag{19}$$

$$\Delta T = \frac{2L}{V} \tag{20}$$

After fault event along with the propagation of the TWs to both sides of the TL, the TW reaches the busbar *N*, and a part of this TW is reflected to the fault point. This TW has the same polarity as incident TW. A part of the TW that reaches the fault point is transmitted toward the busbar *M* as the high-impedance fault occurs. Additionally, the time of the reflected TW can be obtained using the following equation when the i^{th} TW selects the role *B* as below:

$$t_i^A = \frac{2L - Vt_i}{V} \tag{21}$$

Role *C* signifies a player that is a reflected TW from the fault point induced by a fault. The fault location can be obtained using the following equation:

$$EF_i^A = \frac{L \times t_i}{\Delta T} \tag{22}$$

To distinguish the fault location in the first or second half of the TL, role (D) is considered in this paper. This shows the second successful reflection from the fault point. With respect to the faults that occur on the first half of the TL, one of the identified TWs selects role (D). However, if the fault is in the second half at a time interval of ΔT, no TWs select this role. The t_i^A signifies the approximate time in order to notice the reflected TW from a fault point. The accuracy of the estimated time can be evaluated using the search field definition [16].

C) Game Payoff

The strategy profile S_i can yield the TW_i payoff. This can be calculated as follows: The $u_k(TW_i)$ function equals 1 when a TW is observed within the calculated time range; otherwise, it is zero. On the other hand, when the estimated time is out of range, $u_k(a_i)$ function is –1.

Considering $\mathcal{C}$ in the player set, element $\mathcal{C}$ is a coalition that is built up by some players. The players in the coalition seek the same goal and act using an optimal strategy by solving an optimization function.

5 Implementation of the Scheme

5.1 Studied System

The single line diagram for the studied power system is shown in Fig. 10. The test system having four areas connected by the TL of 500 kV. The distributed model signifies the TL, and stray capacitance of 0.01 μF is assumed at each busbar [7]. TL and source parameters are shown in Table 2. The power system is modeled in MATLAB/Simulink. MATLAB software was used to perform the proposed fault protection scheme, analytical evaluation of the signal, and Cooperative game modeling. A UPFC of 100-MVA comprises two- and three-level, as well as 48-pulse GTO-based converter, each of which is linked side to side of the DC capacitors of 2500 μF. The STATCOM is connected through a shunt transformer 15/500 kV in the UPFC. Moreover, the SSSC is connected through a series coupling transformer. It is always preferred to install mid-line. In this paper, the UPFC located at the TL A-B is used to control the active and reactive powers flowing through this TL. The UPFC modeling and its controller are referred from [3].

The signal sampling is performed at a frequency range of 1 MHz [7]. The signals are transformed into distinct modal components using Clark's real transformation matrix [7]. This study utilized the signal mode α to extract TWs using different techniques in papers. It is of significant importance to state that this study did not assess the performance of the TW detectors. Accordingly, it used the mathematical morphology filter and DWT to evaluate the efficiency of the proposed scheme.

Table 2 system data.

TLS		
Voltage	[kv]	500
Positive seq. impedance	[Ω/km]	0.025+j0.3518
Positive seq. shunt capacitive	[nF/km]	12.74
Zero seq. impedance	[Ω/km]	0.3864+j1.554
Zero seq. shunt capacitive	[nF/km]	7.75
System C, D, E, AND F		
Positive seq. impedance	[Ω]	1.43+j16.21
Zero seq. impedance	[Ω]	3.068+j28.746
System frequency	[Hz]	60

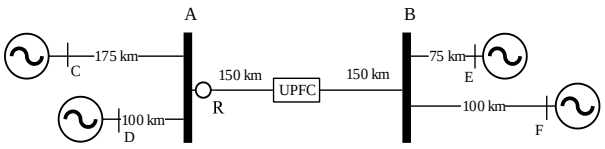

Fig. 10 Model of the simulated system.

6 Simulation Result and Discussion

The identified TWs over ΔT_{record} time for a fault in the second half of the TL are presented in Fig. 11. Moreover, the coalition reveals the roles specified for each player.

6.1 Accuracy Analysis

In total, different fault distances (FD) from the busbar A were utilized to simulate all possible types of faults (FT), namely LG, LLG, LL, and 3LG with a fault resistance (FR) of 0–50 to evaluate the proposed scheme performance. Table 3 summarizes the fault location estimation errors. The maximum error is acceptable for all cases that indicate the accuracy of the proposed scheme.

6.2 Influence of the Fault Impedance and Fault Inception Angle

The effects of fault impedance and fault inception angle variation are investigated on the scheme's accuracy taking into account all possible unbalanced fault types that can be encountered in the TL (Table 3). The faults were investigated in terms of fault impedance values within the range between 0 and 50 Ω. This captures low- and high-resistance faults. Fault detection in small fault inception angle is one of the problems in the existing protection schemes. A fault at the voltage accompanied by a small amplitude leads to the weak amplitude of TWs caused by the fault, thereby reducing the number of detected TWs. This affects the proposed scheme operation. In these conditions, however, the proposed scheme could easily identify the first reflected TW from the fault point to distinguish the TWs. Some simulations were carried out to study the effects of the fault inception angle (Table 3).

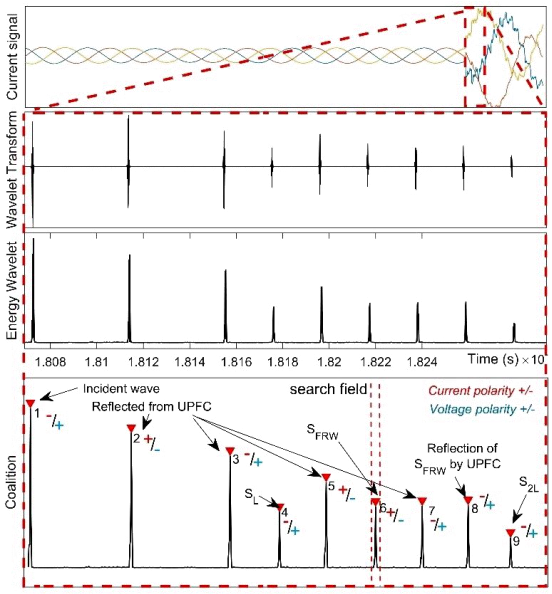

Fig. 11 Identified TWs using coalition for a fault in the second half of the TL (FT: 3LG, FD: 210 km, FR: 10 Ω).

Table 3 Fault location error with varying fault resistance, fault distance, and fault inception angle.

FT	FR [Ω]	FIA [°]	Actual fault location	Faulty section	d_{com}	UPFC references P[pu], Q[pu], V[pu]	$S_{Incident}$ and $K_{threshold}$	$\|S_{FRW}\|$	Internal (I) /External (E) fault	Error [%]
LG	0	0	10	*A-B*	150	9 -0.6 1.005	7.55 2.08	3.42	I	0.01
		15	180	*A-B*		9 -0.6 1.005	17.5 3.97	6.22	I	0.003
		30	210	*A-B*		7 0.5 1.005	7.25 1.72	2.08	I	0.0015
	50	0	305	*B-E*		9 -0.6 1.005	0.139 0.0315	0.0269	E	-
		15	80	*A-B*		7 -0.6 1.005	30.43 6.9	13.08	I	0.052
		30	150	*A-B*		7 0.5 1.005	8 1.82	2.34	I	0.015
LL	0	0	330	*B-F*	150	7 0.5 1.005	6.58 1.5	1.32	E	-
		15	110	*A-B*		9 0.5 1.005	12.1 2.75	3.08	I	0.0001
		30	160	*A-B*		9 0.5 1.005	8.31 1.89	2.12	I	0
	50	0	250	*A-B*		7 -0.6 1.005	7.79 1.77	3.73	I	0.03601
		15	15	*A-B*		9 -0.6 1.005	155.83 35.5	69.8	I	0.02
		30	325	*B-E*		7 -0.6 1.005	2.95 0.672	0.324	E	-
LLG	0	0	290	*A-B*	150	9 0.5 1.005	4.59 1.04	1.17	I	0.0025
		15	60	*A-B*		9 0.5 1.005	22.2 5.05	5.65	I	0.0059
		30	365	*B-F*		9 -0.6 1.005	3.02 0.689	0.39	E	-
	50	0	350	*B-E*		7 0.5 1.005	4.56 1.04	0.958	E	-
		15	20	*A-B*		7 0.5 1.005	101.53 23.1	44.99	I	0.0001
		30	295	*A-B*		9 0.5 1.005	4.37 0.995	1.16	I	0.003
3LG	0	0	25	*A-B*	150	7 -0.6 1.005	105 23.8	36.4	I	0.002
		15	75	*A-B*		9 -0.6 1.005	17.9 4.08	7.21	I	0.0819
		30	400	*B-F*		7 0.5 1.005	2.74 0.623	0.341	E	-
	50	0	370	*B-E*		9 -0.6 1.005	4 0.911	0.881	E	-
		15	30	*A-B*		7 0.5 1.005	81.16 18.5	34.9	I	0.00072
		30	155	*A-B*		7 -0.6 1.005	7.74 1.76	2.27	I	0.00081

6.3 Influence of the UPFC Mode Operation

The number of TWs can be detected after the identification of the first incident TW which relies on the UPFC mode. Accordingly, the outputs are represented in different modes to assess the impact of the UPFC mode modification on the proposed scheme. Obviously, no disturbance is observed in discrimination and fault location of the outputs because of the changes in the detected number of TWs.

6.4 Influence of TW Extraction

Different numbers of TWs can be extracted from the signal using the varieties in the detection techniques. Table 4 tabulates the outputs of the extraction method (i.e., MMF and DWT) to assess the proposed scheme. Based on the output results, the proposed scheme relies on no extraction method. The varieties in the threshold of the extracted algorithms are in an acceptable range; accordingly, this method faces no challenges due to the rational performance of the Cooperative game to discriminate the identified TWs.

6.5 Effect of Error in TL Parameters

Table 5 summarizes the error effect in the TL parameters on the proposed algorithm performance regarding the identification of the external fault. According to the results, in all cases, there is a significant difference between the $K_{threshold}$ and $|S_{2L}|$ in terms of the amplitude; therefore, the error in the TL parameter has no effect on the identification of the fault in the adjacent line or TL. As a result, the performance of the proposed algorithm is not affected by the errors in TL parameters.

6.6 Compensator Location

Table 6 tabulates the performance of the proposed method for altering the UPFC location. Moreover, the results show no dependency of the method on the installation location of the UPFC.

6.7 Comparison With Other Methods

In order to compare the efficiency of the proposed method with the existing approach (based on the TW) the detection and location methods, have been implemented on the UPFC compensated transmission system. All these schemes have been evaluated at the sampling rate of 1 MHz as needed. The results summaries for different fault cases are given in Table 7.

Regarding the TW-based fault location algorithms, the fault location error in [24] and [25] is almost much. However, these two studies have been proposed for the presence of TCSC, and they sometimes encounter wrong performance in the fault location for a fault after the UPFC due to the presence of UPFC and its high switching frequency. On the other hand, [19] and [18] display correct performance for internal fault owing to

Table 4 Average of fault location error with varying extraction technique.

FT	FR [Ω]	FIA [°]	TW extraction method	*A-B* 50 km	*A-B* 20 km	*A-B* 160 km	*A-B* 275 km
LG	0	5	MMF	0.02	0.008	0	0.008
			DWT	0.038	0.008	0.0001	0.0073
LLG	50	30	MMF	0.0001	0.002	0	0.02
			DWT	0.001	0.003	0.0001	0.02

Table 5 error effect in the line and cable parameters on the proposed algorithm performance.

				ꝏ: Inductive mode, ╫: Capacitive mode				
FT	FR [Ω]	FIA [°]	α_{error}	Actual fault location, faulty section	$K_{threshold}$	$\|S_{FRW}\|$	Internal (I) /External (E) fault	UPFC mode
LL	50	15	1.05α	15	35.1	69.8	I	P = 9
			0.95α	*A-B*	35.8		I	Q = -0.6
LG	50	0	1.05α	305	0.0312	0.0269	E	P = 9
			0.95α	*B-E*	0.0319		E	Q = -0.6
LLG	50	30	1.05α	295	2	3.086	I	P = 9
			0.95α	*A-B*	1.01		I	Q = 0.5
LLG	0	30	1.05α	365	0.682	0.39	E	P = 9
			0.95α	*B-F*	0.695		E	Q = -0.6
LL	0	15	1.05α	110	2.73	3.08	I	P = 9
			0.95α	*A-B*	2.78		I	Q = 0.5

Table 6 Average of fault location error with varying compensator location.

FT	FR [Ω]	d_{com} [km]	Actual fault location			
			A-B 15 km	*A-B* 100 km	*A-B* 150 km	*A-B* 280 km
LG	0	50	0.0002	0.0024	0.0001	0.003
LL	30	150	0.034	0.0061	0.0002	0.012
LLG	0	200	0.00024	0.0008	0.0001	0.003
3LG	30	260	0.004	0.0004	0.0002	0.00085

Table 7 Comparison of some TW methods employed for detection and/or location of the fault in FACTS compensated transmission system.

Method	Type of scheme	Purpose/Task	Computational intelligence technique	Compensated device	F1	F2	F3	F4
[24]	Single end	Fault location	DWT	TCSC	○	✓	✗	○
[25]	Single-end	Protection and location	DWT	TCSC	✓	✓	✗	○
[19]	Single-end	Protection and location	MMF and Game theory	TCSC	✓	✓	✓	✗
[18]	Single-end	Protection and location	MMF and Game theory	SVC	✓	✓	✓	○
[26]	Double-end	detection	Wavelet transform	STATCOM	○	✓	✓	○
[9]	Double-end	Fault location	Wavelet transform and fuzzy logic	UPFC	○	✓	✓	○
Proposed method	Single-end	Protection and fault location	DWT and Cooperative game	UPFC	✓	✓	✓	✓

○ Not presented; ✓ Not dead zone; ✗ Has dead zone.
F1: External backward fault, F2: Internal fault (before Compensator), F3: Internal fault (after compensator), F4: External forward fault

high sampling frequency and non-degradation of high-frequency TWs with UPFC production harmonics; however, they face challenges when identifying the external forward fault. In contrast, the double-end algorithms proposed by [26] and [9] performed correctly. It is worth mentioning that these studies proposed no algorithm for external fault detection.

7 Conclusion

The compensators are accompanied by several challenges in the conventional protection methods of TLs. This study aimed to assess the impact of UPFC on the protection scheme using TWs. It is therefore concluded that UPFC controller in TLs results in the reflection of the point of connection, as well as addition of harmonics and transients, thereby leading to the maloperation or disturbance of the proper TW relay operation. To increase the efficiency of the total TL protection and stop unwanted tripping of the breaker in the presence of UPFC devices compensator, a novel protection scheme is introduced to protect and locate the fault based on the TW using the cooperative Game and extraction technique. Furthermore, the results demonstrated no effects of the UPFC and its mode on the proposed scheme performance. The simulation results revealed that the proposed scheme did not rely on no fault location, fault type, fault impedance, and fault inception angle. Furthermore, the MMF and DWT techniques were used to extract the TWs and evaluate the proposed scheme efficiency. According to the findings of the study, a difference was observed between the MMF and DWT methods in terms of the number of extracted TWs. In the same vein, the output findings of both extraction methods indicated the accurate performance of the proposed method considering different numbers of the extracted TWs resulted from the Cooperative Game structure. This showed that the proposed method was not dependent on the number of the extracted TWs and existing thresholds of the extraction methods.

The proposed method requires a TW velocity estimation algorithm to improve error fault location. On the other hand, due to the fact that this method is single-end, its dependence on TL parameters will be higher than double-end method. The proposed method operates at 1 MHz practical sampling frequency. This sampling rate limits the proposed algorithm to fault location from a distance of 200 m to the local end of the TL. The sampling rate should be increased to locate the fault at a closer distance without TW interference.

Intellectual Property

The authors confirm that they have given due consideration to the protection of intellectual property associated with this work and that there are no impediments to publication, including the timing of publication, with respect to intellectual property.

Funding

No funding was received for this work.

CRediT Authorship Contribution Statement

M. Khalili: Idea & conceptualization, Research & investigation, Analysis, Methodology, Software and simulation, Original draft preparation, Revise & editing. **F. Namdari:** Idea & conceptualization, Supervision, analysis, Project administration, Verification, original draft preparation, Revise & editing. **E. Rokrok:** Idea & conceptualization, Data curation, Analysis, Supervision, verification.

Declaration of Competing Interest

The authors hereby confirm that the submitted manuscript is an original work and has not been published so far, is not under consideration for publication by any other journal and will not be submitted to any other journal until the decision will be made by this journal. All authors have approved the manuscript and agree with its submission to "Iranian Journal of Electrical and Electronic Engineering".

References

[1] F. A. Albasri, T. S. Sidhu, and R. K. Varma, "Performance comparison of distance protection schemes for shunt-FACTS compensated transmission lines," *IEEE Transactions on Power Delivery*, Vol. 22, No. 4, pp. 2116–2125, 2007.

[2] S. Biswas and P. K. Nayak, "State-of-the-art on the protection of FACTS compensated high-voltage transmission lines: A review," *High Voltage*, Vol. 3, No. 1, pp. 21–30, 2018.

[3] S. K. Mishra and L. N. Tripathy, "A critical fault detection analysis & fault time in a UPFC transmission line," *Protection and Control of Modern Power Systems*, Vol. 4, No. 3, pp. 1–10, 2019.

[4] A. Ghorbani, S. Y. Ebrahimi, M. Ghorbani, "Active power based distance protection scheme in the presence of series compensators," *Protection and Control of Modern Power Systems*, Vol. 2, No. 7, pp. 1–13, 2017.

[5] A. N. Alsammak, S. Arkan, "Enhancement effects of the STATCOM on the distance relay protection," *International Journal of Computer Applications*, Vol. 182, No. 40, pp. 10–14, 2019.

[6] F. Deng, X. Zeng, and L. Pan , "Research on multi-terminal traveling wave fault location method in complicated networks based on cloud computing platform," *Protection and Control of Modern Power Systems*, Vol. 2, No. 19, pp. 1–12, 2017.

[7] F. Namdari and M. Salehi , "High-speed protection scheme based on initial current traveling wave for transmission lines employing mathematical morphology," *IEEE Transactions on Power Delivery*, Vol. 32, No. 1, pp. 246–253, 2017.

[8] A. M. El-Zonkoly and H. Desouki, "Wavelet entropy based algorithm for fault detection and classification in FACTS compensated transmission line," *International Journal of Electrical Power & Energy Systems*, Vol. 33, No. 8, p. 1368–1374, 2011.

[9] R. K. Goli, A. G. Shaik, and S. S. T. Ram, "A transient current based double line transmission system protection using fuzzy-wavelet approach in the presence of UPFC," *International Journal of Electrical Power & Energy Systems*, Vol. 70, p. 91–98, 2015.

[10] B. Kumar and A. Yadav, "Wavelet singular entropy approach for fault detection and classification of transmission line compensated with UPFC," in *International Conference on Information Communication and Embedded Systems (ICICES)*, pp. 1–6, 2016.

[11] M. Ebeed, S. Kamel, J. Yu, and F. Jurado, "Development of UPFC operating constraints enforcement approach for power flow control," *IET Generation, Transmission & Distribution*, Vol. 13, No. 20, pp. 4579–4591, 2019.

[12] Z. Li, Y. Cheng, X. Wang, Z. Li, and H. Weng, "Study on wide-area traveling wave fault line selection and fault location algorithm," *International Transactions on Electrical Energy Systems*, Vol. 28, No. 12, 2018.

[13] R. U. Pote, G. K. Mahajan, and G. P. Tembhurnikar, "Analysis of T-STATCOM-6, 12, 48 Pulse," *International Journal for Modern Trends in Science and Technology*, Vol. 4, No. 12, 2018.

[14] D. M. Mohan, B. Singh, B. K. Panigrahi, "A Two-Level, 48-Pulse Voltage Source Converter for HVDC Systems," in *Fifteenth National Power Systems Conference (NPSC)*, Bombay, 2008.

[15] L. Tang, X. Dong, S. Luo, S. Shi, and B. Wang, "A new differential protection of transmission line based on equivalent travelling wave," *IEEE Transactions on Power Delivery*, Vol. 32, No. 3, pp. 1359–1369, 2017.

[16] F. V. Lopes, K. M. Dantas, K. M. Silva, B. Costa, "Accurate two-terminal transmission line fault location using traveling waves," *IEEE Transactions on Power Delivery*, Vol. 33, No. 2, pp. 873–880, 2018.

[17] F. V. Lopes and D. Fernandes, "A traveling-wave detection method based on Park's transformation for fault locators," *IEEE Transactions on Power Delivery*, Vol. 28, No. 3, pp. 1626–1634, 2013.

[18] M. Khalili, F. Namdari, and E. Rokrok, "Traveling wave-based protection for SVC connected transmission lines using game theory," *International Journal of Electrical Power & Energy Systems*, Vol. 123, 2020.

[19] M. Khalili, F. Namdari, and E. Rokrok, "Traveling wave-based protection for TCSC connected transmission lines using game theory," *International Journal of Electrical Power & Energy Systems*, Vol. e12545, 2020.

[20] S. Sivanagaraju and S. Satyanarayana, *Electric power transmission and distribution*. Pearson Education India, 2008.

[21] S. Mei, W. Wei, and F. Liu, "On engineering game theory with its application in power systems," *Control Theory and Technology*, Vol. 15, No. 1, pp. 1–12, 2017.

[22] S. Abapour, M. Nazari-Heris, B. Mohammadi-Ivatloo, and M. Tarafdar Hagh, "Game theory approaches for the solution of power system problems: A comprehensive review," *Archives of Computational Methods in Engineering*, Vol. 27, pp. 81–103, 2018.

[23] X. Zheng, H. Chen, C. He, W. Mo, and Y. Chen, "Cooperative game model for power system secondary voltage control," in *IEEE PES Asia-Pacific Power and Energy Engineering Conference*, Xi'an, 2016.

[24] E. Reyes-Archundia, C. Cardoso-Isidoro, J. A. Gutirrez-Gnecchi, J. A. Gutiérrez-Gnecchi, G. M. Chávez-Campos, and J. Correa-Gómez, "Algorithm based on microntroller for high speed protection in compensated transmission line," in *IEEE International Autumn Meeting on Power, Electronics and Computing (ROPEC)*, pp. 1–6, 2016.

[25] E. Reyes-Archundia, E. Moreno-Goytia, and J. Guardado, "An algorithm based on traveling waves for transmission line protection in a TCSC environment," *International Journal of Electrical Power & Energy Systems*, Vol. 60, p. 367–377, 2014.

[26] P. V. Rao, S. A. Gafoor, and C. Venkatesh, "Detection of transmission line faults in the presence of STATCOM using wavelets," in *Annual IEEE India Conference*, Hyderabad, pp. 1–5, 2011.

M. Khalili was born in Khomein, Iran, 1989. He received B.Sc. degree in Electrical Power Engineering from Kermanshah University of Technology, Kermanshah, Iran, in 2012 and M.Sc. degree from Tafresh University, Tafresh, Iran, in 2014 and Ph.D. in 2021 at the Lorestan University. His areas of interest include microgrid operation and protection, artificial intelligence, traveling wave protection, power system protection, and smart grid.

F. Namdari was born in Khoramabad, Iran, 1972. He received his B.Sc. in 1995 at the Iran University of Science and Technology (IUST), M.Sc. in 1998 at the Tarbiat Modarres University (TMU), Iran, and Ph.D. in 2006 at the IUST all in Electrical Power Engineering. He is an Associate Professor with the Department of Electrical Engineering at Lorestan University, Khoramabad, Iran. His areas of interest include power system protection, smart grids, power system operation and control, and artificial intelligence (AI) techniques in power systems.

E. Rokrok was born in Khoramabad, Iran, 1972. He received his B.Sc., M.Sc., and Ph.D. degrees in Electrical Engineering from Isfahan University of Technology, in 1985, 1997, and 2010, respectively. He is an Assistant Professor in the Department of Electrical Engineering, Lorestan University, Khoramabad, Iran. His major research interests lie in the area of power system control and dynamics, dispersed generation, microgrid, power electronic, and robust control.